Chemometric investigations of the multidrug resistance in strains of the phytopathogenic fungus *Penicillium digitatum*

Márcia Miguel Castro Ferreira and Rudolf Kiralj. ***marcia@iqm.unicamp.br, rudolf@iqm.unicamp.br, http://lqta.iqm.unicamp.br***
Laboratório de Quimiometria Teórica e Aplicada (LQTA), Instituto de Química, Universidade Estadual de Campinas, Campinas SP, 13084-971, Brazil

THE OBJECTIVES OF THIS WORK

1) ***P. digitatum*** **(green mold), like other** ***Penicillium*** **species, contaminates fruits, nuts, vegetables, and even cereals causing serious losses in agriculture worldwide, and various respiratory problems, allergic diseases and other non-inflammatory symptoms that may be extremely dangerous to immunocompromised persons. To get more insight into the multidrug resistance (MDR) mechanisms of this microbe, particularly CYP51- (cytochrome 51 – ergosterol biosynthesis) and efflux pump PMR1-mediated resistance to demethylation inhibitors (DMIs), is one of the objectives;**

2) **To present novel ASR (Activity- Structure Relationship) & chemometric study of MDR activities of diverse** ***P. digitatum*** **strains with respect to DMIs;**
3) **To present novel QGAR (Quantitative Genome-Activity Relationship) and regression modeling of these MDR activities, taking into account the genome structure of the strains.**

GENERAL: THE MOLD AND ITS ANTIFUNGALS

1

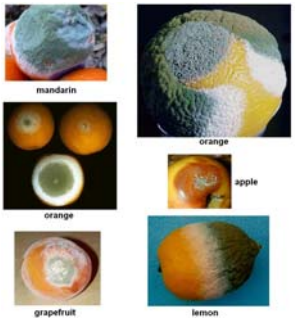

The most frequent targets of ***P. digitatum*** **are fruits, especially citric fruits (photos from WWW resources).**

P. digitatum **under microscope (photos from WWW resources). The brush-like heads (Lat. penicillus = brush) have finger-like shape (Lat. digitatum = fingered) at their spore-producing ends.**

2

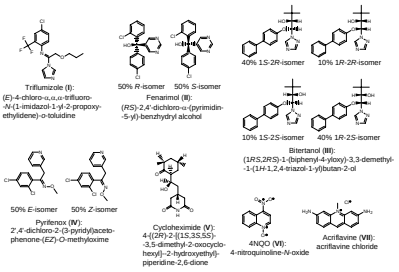

Molecular structure & isomeric composition of commercial agents used as azole-based fungicides (DMIs: I-IV), an antibiotic (V) and mutagens (VI, VII). These resistance of ***P. digitatum*** **strains against these compounds is studied in this work. The activity data are MIC (Minimal Inhibitory Concentration) and EC_{50} (Effective Concentration for 50% radial growth inhibition) from literature: R. Nakaune et al, Microbiol. 64 (1998) 3983; H. Hamamoto et al., Appl. Env. Microbiol. 66 (2000) 3421; H. Hamamoto et al., Pestic. Biochem. Physiol. 70 (2001) 19; H. Hamamoto et al., Pest Manag. Sci. 57 (2001) 839; R. Nakaune et al., Mol. Genet. Genom. 267 (2002) 179. Below is the mean radial growth of fungal cultures as a function of concentration (EC_{50} and MIC, reconstructed plot).**

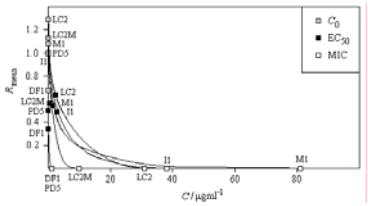

ACTIVITY-STRUCTURE RELATIONSHIPS (ASR) I

3

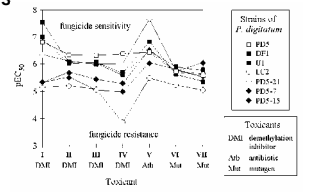

Biological activities were used as pMIC=-log[MIC/mol dm^{-3}] and pEC50=-log[E50/mol dm^{-3}], and also as relative to the standard strain (PD5): $pECr_{50}=pEC_{50}(PD5)-pEC_{50}$. Strains PD5, DF1 and LC2 are sensitive to DMIs (DMI-S), LC2 is resistant to DMIs (DMI-R), and other strains are moderately resistant (DMI-M).

5

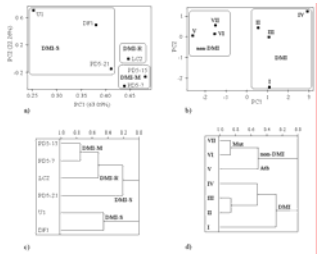

Exploratory analysis of the data set A2 (7x6 matrix of $pECr_{50}$: 7 toxicants and 6 strains). a) PCA loadings plot shows the clustering of the ***P. digitatum*** **strains. b) PCA scores plot shows the clustering of the toxicants. c) HCA dendrogram for variables ($pECr_{50}$) and the clustering of the** ***P. digitatum*** **strains; d) HCA dendrogram for the samples (toxicants) and their clustering. Observations similar to those from the previous analysis can aid in designing new antifungals against strains with elevated MDR (Multidrug Resistance) to known fungicides.**

4

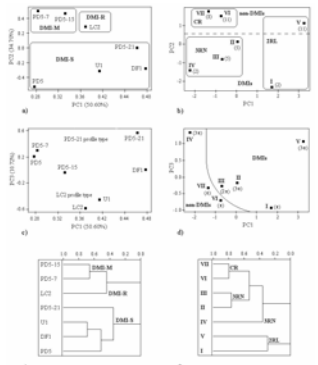

Exploratory analysis (PCA – Principal Component Analysis and HCA – Hierarchical Cluster Analysis) of the data set A1 (7x7 matrix of pMICs: 7 toxicants and 7 strains). a) PCA loadings plot shows the clustering of the ***P. digitatum*** **strains. b) PCA scores plot shows the clustering of the toxicants with the number of hydrogen bonds and charge-charge interactions in brackets. c) Other PCA loadings plot shows the distribution of the** ***P. digitatum*** **strains with respect to the profile types from the previous Figure. d) PCA scores plot shows the clustering of the toxicants with the number of π-systems in brackets. e) HCA dendogram for variables (pMICs) and the clustering of the** ***P. digitatum*** **strains; f) HCA dendogram for the samples (toxicants) and their clustering. The samples are classified as condensed ring systems (CR: Mut toxicants VI and VII), two-ring linear systems (2RL: I and V), and three-ring non-linear systems (3RN: II, III, and IV with bent topology that mimics a three-ring structure). PC1 makes some distinction between DMIs and non-DMIs. The increase in PC1 is related to higher molecular flexibility and lower compactness. The increase in PC2 is related to the elevated number of hydrogen bonds and polar character. These observations may be useful in discovering new antifungals.**

ACTIVITY-STRUCTURE RELATIONSHIPS (ASR) II

6

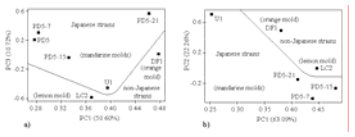

PCA loadings plots showing the discrimination of the ***P. digitatum*** **strains with respect to their origin (Japanese or non-Japanese) and target citric fruit (orange, mandarin and lemon mold): a) exploratory analysis of the dataset A1; b) exploratory analysis of the dataset data set A2.**

7

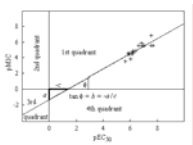

Definition of the dataset A3. Linear regression relationship pMIC = $a + b$ pEC_{50} using experimental data (all measurements and strains available) for each toxicant (I-VII) gives five descriptors: a, b, c, $|a|$ and $|c|$. These data make matrix 7X5 (7 toxicants and 5 descriptors).

8

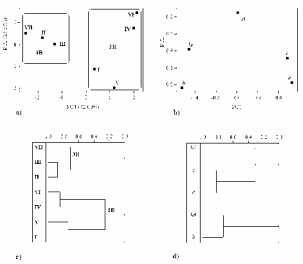

Exploratory analysis of the data set A3: a) PCA scores plot shows the clustering of the toxicants. b) PCA loadings plot shows the clustering of the variables. c) HCA dendogram for the samples (toxicants) and their clustering; d) HCA dendogram for variables. There is a cluster of molecules with three rings (3R, more compact structures), and the other one of molecules with two rings (2R, less compact structures). Molecular compactness decreases along PC1 and increases along PC2. This property can be used to predict values of the descriptors, and hence, the toxicant activity against ***P. digitatum*** **strains.**

9

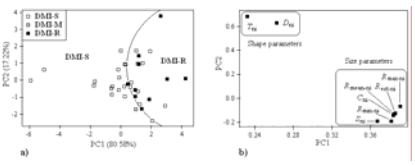

Dataset B1 obtained from measurements of fungal culture photographs in absence of toxicants was used to form matrix 39x8 (39 strains and 8 morphological descriptors: radii R, circumferences C and surface areas S of the cultures). Exploratory analysis: a) PCA scores plot shows the tendency in discrimination of DMI-S from DMI-R strains; b) PCA loadings plot shows the groups of fungal morphology (shape and size) descriptors. Better discrimination of DMI-S from DMI-R strains may be obtained by introducing new descriptors.

Dataset B obtained by extension of the B1 with 8 analogue descriptors for fungal cultures in presence of triflumizole. This gave matrix 39x16. The PCA scores plots: a) strains discriminated according to their baseline DMI resistance character; b) strains distributed according to their geographic origin; c) strains differentiated by their target types (fruits). This discrimination is rather satisfactory. New methods would be desirable that only bioassays without toxicants would be sufficient to identify the strains and their MDR character and other characteristics.

10

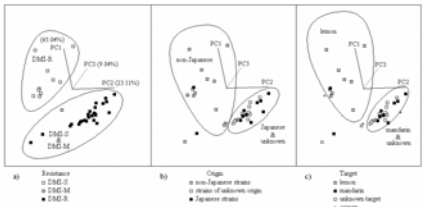

QUANTITATIVE GENOME-ACTIVITY RELATIONSHIPS (QGAR)

11

Genome descriptors:
PMR1-g – presence or absence of the native functional (non-disrupted) ***PMR1*** **gene, or the presence of a** ***PMR1*** **gene from another plasmid;**
PMR1-e – constitutive ***PMR1*** **gene expression level (quantity of total RNA) in the absence of a toxicant, relative to DMI-S strains;**
PMR-t – *PMR1* expression level (quantity of total RNA) induced by a toxicant, triflumizole;
PCR – the size of the promoter fragment in the *PdCYP51* gene, corresponding to one or more copies of the *CYP51* transcriptional enhancer;
CYP51-e – constitutive *CYP51* gene expression level (quantity of total RNA) in the absence of a toxicant, relative to DMI-S strains;
CYP51-g – the number of the transcriptional enhancer copies in the *CYP51* gene.

The dataset C1 (matrix 92x6 with 6 descriptors and vector 92x1 for pEC_{50}) was formed from these descriptors and corresponding MDR activities obtained from 92 experiments with 24 diverse strains and DMI toxicants I-IV. The dataset C2 (matrix 29x6 with the descriptors and vector 29x1 for pEC_{50}) was formed in the same way for non-DMI toxicants V-VII. The complete data set C (matrix 131x6 with descriptors and vector 131x1 for pEC_{50}) was made of C1 and C2.

12

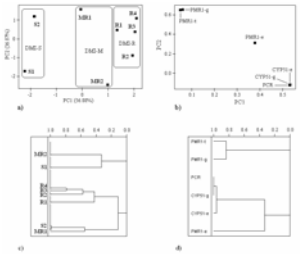

Exploratory analysis of the six genome variables (the data set C1): a) PCA scores plot shows the clustering of the ***P. digitatum*** **strains. b) PCA loadings plot shows the clustering of the genome variables. c) HCA dendogram for samples, showing eight cases of the variable combinations; d) HCA dendogram for variables. A new classification scheme of** ***P. digitatum*** **strains introduces some differences with respect the the previous classification: S1 class contains the most DMI-susceptible strains with no functional** ***PMR1*** **gene and only one copy of the** ***CYP51*** **gene enhancer. The most DMI-resistant class R4 has completely functional** ***PMR1*** **and 5 copies of the** ***CYP51*** **enhancer. Moderately resistant classes (MDR1, MDR2) lie between S- and R-classes. The present analysis shows that the DMI-resistance character, although mainly being determined by the CYP51 resistance mechanism, is also affected by the PMR1 resistance mechanism.**

QGAR using PLS (Partial Least Squares) regression for the C1 data set showed to have satisfactory statistics, and therefore, can be used in further predictions of strain/toxicant behavior: 99.45% in 3 PCs, R = 0.898, Q = 0.888, SEV = 0.339, SEP = 0.333, 6 outliers removed.

ACKNOWLEDGEMENT: FAPESP